Oct 26th, 12:00 AM

Longwave Buckling of Cold-formed Steel Studs Using Direct Strength

Thomas Sputo

Eighteenth International Specialty Conference on Cold-Formed Steel Structures
Orlando, Florida, U.S.A, October 26 & 27, 2006

Longwave Buckling of Cold-Formed Steel Studs Using Direct Strength

Thomas Sputo[1] and Jennifer Tovar[2]

Abstract

A study to develop methods of analyzing perforated, axially loaded, cold-formed steel studs using the provisions of the Direct Strength Method was undertaken using the Finite Strip Method as the method for determining the elastic buckling stresses. Several different models were developed to represent the effect the web perforations in typical C-section studs. The capacities predicted using the Direct Strength Method for the limit state of longwave buckling were compared to capacities calculated using the equations contained in the AISI *Specification*. For the studs considered in this study, it was confirmed that the effects of the perforations may be neglected for calculating the elastic longwave buckling stress. Strong interaction of distortional buckling modes with long wave buckling was observed and the influence of this interaction is discussed and evaluated. The validity of the results is discussed and recommendations are made for the use of the Direct Strength Method for these members.

Introduction

The cold-formed steel wall stud is a commonly used member, replacing wood studs in light and medium frame construction. Usually manufactured as a lipped C-member (Figure 1), these sections are available in a range of sizes with either solid or perforated webs (Figure 2). Accurate prediction of how these perforations affect member capacity is necessary for safe design.

[1] Senior Lecturer, Department of Civil and Coastal Engineering, 365 Weil Hall, University of Florida, Gainesville, FL 32611; Structural Engineer, Sputo and Lammert Engineering, 10 SW 1st Avenue, Gainesville, FL 32601 (email: sputo@ufl.edu)

[2] Graduate Student, Department of Civil, Architectural and Environmental Engineering, University of Texas, Austin, Texas 78712-0273; Formerly Undergraduate Student, Department of Civil and Coastal Engineering, 365 Weil Hall, University of Florida, Gainesville, FL 32611 (email: jennifer@schwabse.com)

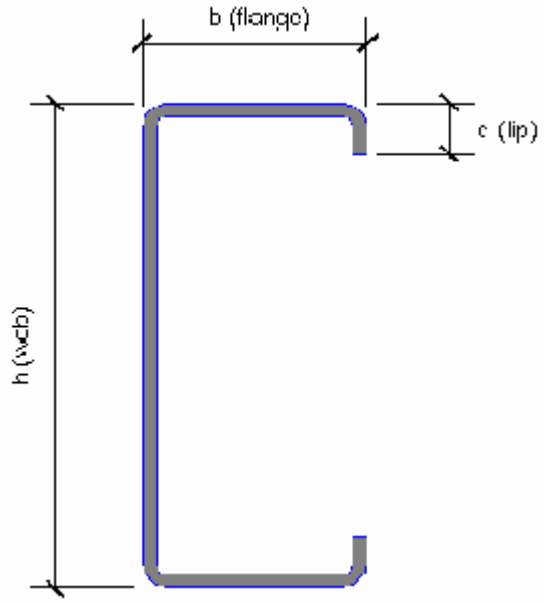

Figure 1. Typical C-stud Cross-section.

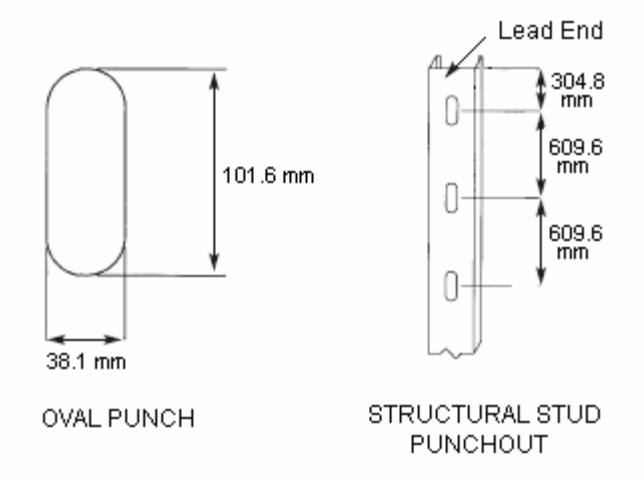

Figure 2. Typical Punchout Dimensions

Current AISI Provisions for Longwave Buckling

The main section of the AISI *Specification for the Design of Cold-Formed Steel Structural Members* (2004) contains provisions for calculating the axial compression capacity of a lipped channel in section C4. These provisions account for longwave buckling in the form of flexural, torsional, and flexural-torsional buckling modes. They also provide for the interaction of local buckling with longwave buckling. The longwave buckling capacity is based on a solid section, whereas local buckling is based on an effective section which considers the perforation to exist for the full length of the member.

Direct Strength Method

The *Design of Cold-Formed Steel Structural Members Using the Direct Strength Method* (Schafer, 2002a) is contained as Appendix 1 to the AISI *Specification* (2004). These provisions are applicable for determining nominal axial compression (P_n) and flexural (M_n) strengths of cold-formed steel members. The Direct Strength Method (DSM) of design does not currently include members with perforations, which must be evaluated by the procedures in main body of the Specification or by other rational analysis.

The DSM requires that elastic buckling loads be calculated for longwave buckling (P_{cre}) from the applicable elastic buckling stresses. The Finite Strip Method (FSM) is a recommended numerical method for determining the critical stress for each mode.

The input required for FSM analysis is greatly reduced from that of the Finite Element Method (FEM) because only the basic member cross-section needs to be defined. “Strips” are uniformly defined along the length of the member rather than broken into incremental pieces. The drawback, however, is that members which contain perforations along the length are defined as uniform along the length (e.g., at the perforation (removed), away from the perforation (solid), or an average (equivalent thickness) of these two).

Despite the present complication of defining perforation effects, the FSM is currently the analysis method of choice for the Direct Strength Method. By simplifying the required user input and producing results within a matter of seconds, the FSM becomes a more “user friendly” tool for the designer. Consequently, the development of a FSM model to analyze perforated cold-formed steel sections that reasonably accurately accounts for the effects of common perforations could be advantageous. The Cornell University Finite

Strip Method (CUFSM) is a finite strip method computer software available as freeware and was used to perform this analysis.

Longwave Buckling (Flexural, Torsional, or Torsional-Flexural)

Longwave buckling modes include: flexural buckling (weak axis), torsional buckling, and torsional-flexural buckling (torsion combined with strong axis flexure). See Figures 3, 4, and 5 for illustrations of these modes. Longwave buckling modes occur at half-wavelengths that exceed 4 times the web depth. Some sections may display more than one of these buckling modes as the half-wavelength increases. The critical stress should be evaluated at the lowest elastic buckling stress, which will usually occur at a half wavelength equal to the unbraced length of the column. For example, the critical stress of a 2438 mm column would be selected at a half-wavelength of 2438 mm if completely unbraced and at 1219 mm if braced at the midpoint.

The critical elastic load, P_{cre}, for longwave buckling may be obtained from

$$P_{cre} = F_{cre} * A_g \qquad \text{(Eq. 1)}$$

where F_{cre} = Critical buckling stress for longwave buckling
A_g = Gross area of the section

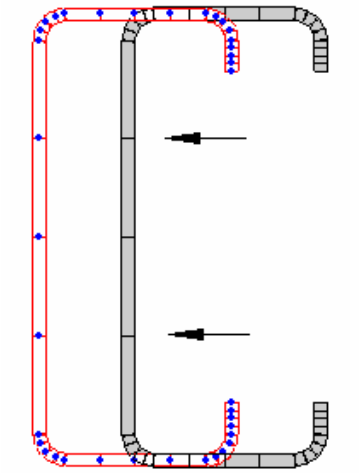

Figure 3. Flexural Buckling: translation in weak axis direction.

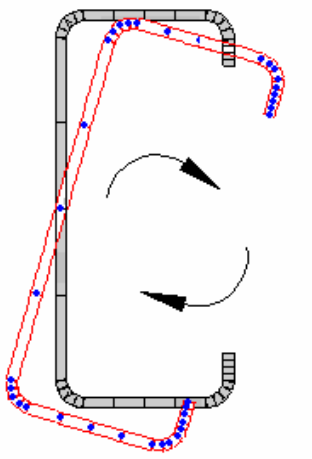

Figure 4. Torsional Buckling: rotation about section center (symmetrical axis).

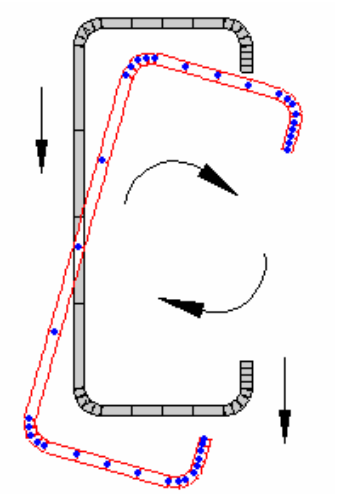

Figure 5. Torsional-Flexural Buckling: uniform rotation and strong axis translation.

The nominal axial strength, P_{ne}, for flexural, torsional, or torsional-flexural buckling is determined by:

for $\lambda_c \le 1.5$ $P_{ne} = \left(.658^{\lambda_c^2}\right) P_y$ (Eq. 2)

for $\lambda_c > 1.5$ $P_{ne} = \left(\frac{.877}{\lambda_c^2}\right) P_y$ (Eq. 3)

where $\lambda_c = \sqrt{P_y / P_{cre}}$ (Eq. 4)

$P_y = A_g F_y$ (Eq. 5)

P_{cre} = Minimum of the critical elastic column buckling load for flexural, torsional, or torsional-flexural buckling according to the elastic buckling stress.

Analysis Procedures

Limitations of Analysis

The sections used for this analysis were restricted to SSMA standard C-shaped cold-formed steel stud cross-sections that are typically used in axial load bearing

conditions. Only axial compression loading was considered. Data was recorded for local, distortional, and longwave buckling for unbraced lengths of 1219 mm and 2438 mm. Yield strengths of both 227.5 and 344.7 MPa were considered. See Table 1 for a complete list of studs considered in this study.

Table 1. Sections Considered in this Study

SSMA Designation	Web Depth D (mm)	Flange Width b (mm)	Lip Length l (mm)	Min. Thick t (mm)
362S162-33	91.07	41.3	12.7	0.84
362S162-43	91.07	41.3	12.7	1.09
362S162-54	91.07	41.3	12.7	1.37
362S162-68	91.07	41.3	12.7	1.73
362S162-97	91.07	41.3	12.7	2.46
600S162-43	152.4	41.3	12.7	1.09
600S162-54	152.4	41.3	12.7	1.37
600S162-68	152.4	41.3	12.7	1.73
600S162-97	152.4	41.3	12.7	2.46
800S162-43	203.2	41.3	12.7	1.09
800S162-54	203.2	41.3	12.7	1.37
800S162-68	203.2	41.3	12.7	1.73
800S162-97	203.2	41.3	12.7	2.46
600S250-43	152.4	63.5	15.9	1.09
600S250-54	152.4	63.5	15.9	1.37
600S250-68	152.4	63.5	15.9	1.73
600S250-97	152.4	63.5	15.9	2.46
800S250-43	203.2	63.5	15.9	1.09
800S250-54	203.2	63.5	15.9	1.37
800S250-68	203.2	63.5	15.9	1.73
800S250-97	203.2	63.5	15.9	2.46

Note: Dimensions given are outside dimensions

Cross-Section Models

Three different cross-section models were used for studying longwave buckling in this study. They are described here in more detail.

Solid Web Model

The baseline model for each section was a solid cross-section without web perforation (Figure 6). This model was selected to provide a reference from

which to judge any modifications, and to represent the response of the member at locations away from the web perforations.

Equivalent-Thickness Model

The most common stud perforation profile includes web perforations 101.6 mm long and 38.1 mm wide, located at 609.6 mm on center along the length of the web (see Figure 2). Therefore, every 609.6 mm segment of stud consists of 508 mm of unperforated web, and only 101.6 mm of perforation. As shown in Figure 7, the removed material from each punch-out was averaged along the web by reducing the web thickness (at a centered 38.1 mm width) by a factor of 0.833. This value is determined as (609.6 – 101.6)/609.6 = 0.833.

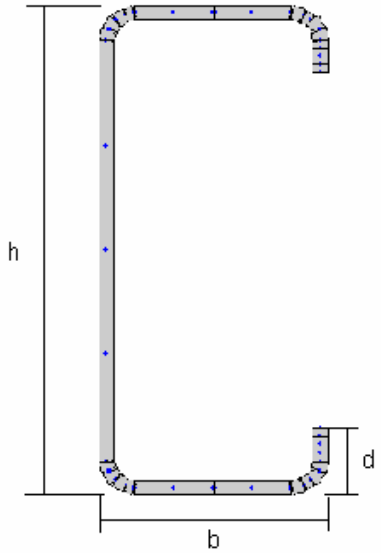

Figure 6. Solid Web Model

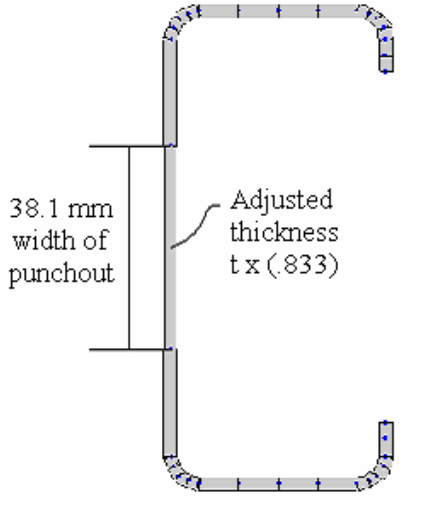

Figure 7. Equivalent-Thickness Model

Perforated Model

For consideration of local buckling, the AISI *Specification* requires that the entire portion of the web along the punchout be ignored in analysis. The perforated model meets this criterion. Because this creates two independent cross-sections, only one-half of the model was used to determine the critical buckling stresses (Figure 8). This critical buckling stress was later applied to the gross area of the full section for strength calculations.

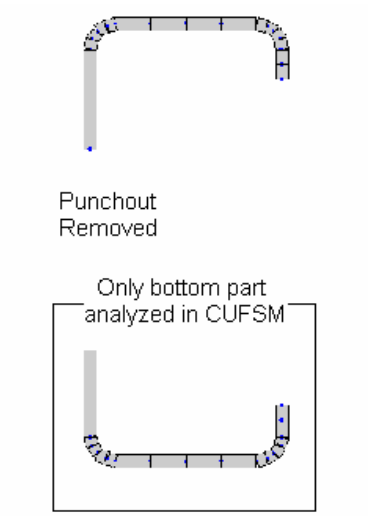

Figure 8. Perforated Web Model

Analysis Output and Plots

For each section, the results from CUFSM are displayed in the form of a buckling curve for the cross-section being analyzed. This curve (Figure 9) depicts the transition and interaction of buckling modes by plotting load factor vs. half-wavelength. CUFSM marks any local minima along the curve, indicating a least energy critical buckling stress for that mode.

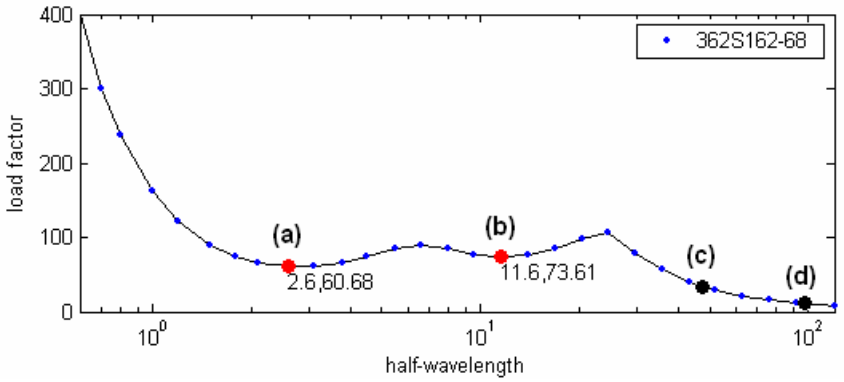

Figure 9. CUFSM section model analysis output for 362S162-68
(Figure units in English system)

Longwave Buckling

The portion of the buckling curve reflecting the longwave buckling mode maintains a downward slope with the increase of half-wavelength. The critical buckling stress for the longwave mode is taken at a half-wavelength equal to the effective unbraced length of the column. For this study, longwave buckling stresses were selected at 1219 and 2438 mm.

For the majority of sections analyzed, these half-wavelengths occurred in the downward slope of the longwave buckling range. It is important to note however, that when either of these half-wavelengths falls near the local maxima between distortional and longwave buckling, there will be heavy (if not dominating) distortional effects, resulting in a buckling mode which is not purely longwave (Figure 10). Schafer (2002b) has noted this interaction to not be of significant concern.

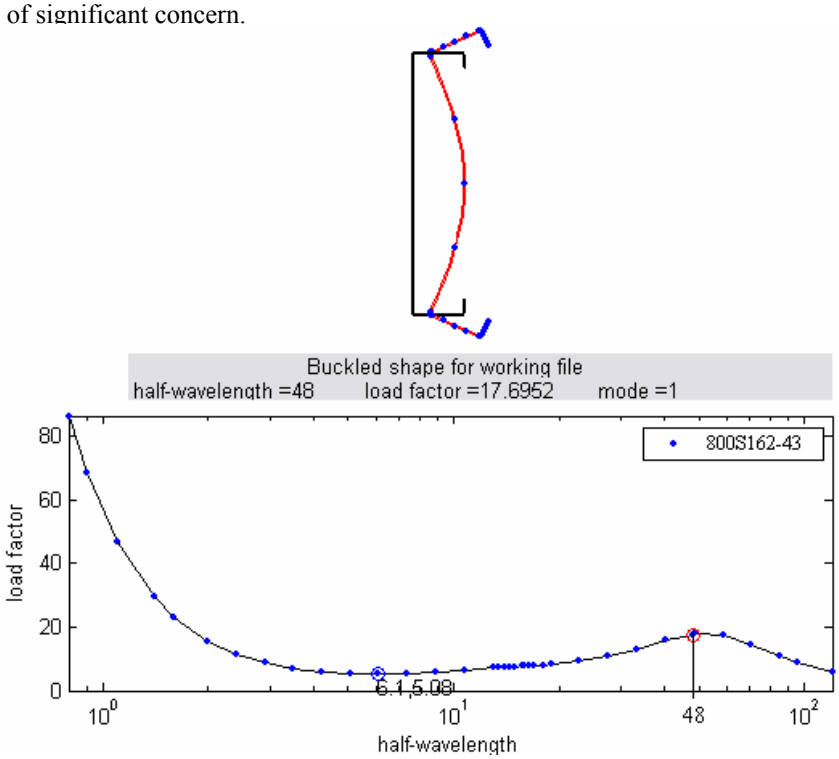

Figure 10. Weak Axis Flexure (Longwave) with Distortional Buckling Interaction where half-wavelength of 1219 mm falls near local maxima for 800S162-43 (Figure units in English system)

Distortional Interaction - Longwave Buckling Results

Distortional buckling interaction with longwave buckling was more noticeable in 600S and 800S studs, and was considerably more significant in studs with 250 flange widths. The distortional bucking was most pronounced at the 1219 mm unbraced length. Refer to Sputo and Tovar (2005) for a tabulation of this interaction for individual stud results.

Longwave buckling was not the controlling buckling state for any of the studs with strong distortional buckling mode interaction. It is important to note, however, that the local buckling strengths for these studs with more slender web height to thickness ratios are not well predicted by the current AISI equivalent width method (Tovar and Sputo, 2006).

Solid Web Model - Longwave Buckling Results

The solid web model is the base model for analysis and is applicable to the calculation of longwave buckling strength, as predicted by the DSM and the current AISI provisions. For an illustration of the solid model refer to Figure 6. Summarized tabulated results for longwave buckling in the solid model can be found in Table 2. Complete results for this limit state are found in Sputo and Tovar (2005).

Table 2. Solid Web Longwave Buckling Summary

Section Criteria	Statistic	DSM/AISI
162 Flange	**Mean**	1.031
	St Dev	0.055
250 Flange	**Mean**	1.057
	St Dev	0.075
All Sections	**Mean**	1.035
	St Dev	0.058

For cases where longwave buckling is the controlling buckling mode, DSM predictions were compared to capacities predicted by the AISI *Specification*. The DSM strength calculations compared favorably with AISI predictions for the solid model.

Equivalent-Thickness Model - Longwave Buckling Results

The equivalent-thickness model was developed to distribute the effects of the holes along the length of the stud. Longwave buckling occurs at a half-wavelength equal to the unbraced length of the member. Standard perforations of 101.6 mm in length are separated by 508 mm of solid web. When investigating unbraced lengths of 1219 and 2438 mm, these lengths encompass two or four perforations, but more significantly, a total of 1016 or 2032 mm of solid material. The equivalent-thickness model takes into account both the perforations and the solid material along the length of the web by averaging the thickness of material applied at the punchout width by a factor of 0.833. The equivalent-thickness model is therefore an applicable model to account for perforations in the prediction of longwave buckling.

Summarized tabulated results for longwave buckling capacity of the equivalent-thickness model as compared to the solid web model are found in Table 3. More comprehensive tabular results are given in Sputo and Tovar (2005). Buckling capacities for the equivalent-thickness model are compared to the solid web model and AISI predictions in Table 4, which is subdivided by different section criteria as noted.

Table 3. Summarized Longwave Buckling Stress Comparison for Equivalent-Thickness and Solid Web

Stud Series	Equivilent Thickness / Solid Web	
	MEAN	**ST DEV**
362S162	0.996	0.011
600S162	0.994	0.023
800S162	0.981	0.035
600S250	0.959	0.055
800S250	0.953	0.048
Total	0.978	0.040

The critical load for longwave buckling was calculated using Eq. 1, where the critical buckling stress is multiplied by the area of the cross-section. The critical buckling stress for this model is predicted using a cross-section with the perforated width of the web reduced by a factor of 0.833. Two separate nominal capacities (P_n) were calculated; one using the full gross cross-sectional area (A_g), and the other using the area obtained from the reduced equivalent thickness web area (A_e). Both these capacities are noted in Table 4.

Table 4. Longwave Buckling Strength Comparison Summary for DSM Equivalent-Thickness and Solid Web with AISI

Section Criteria	Statistic	Equiv-Thick vs. Solid Comparison		AISI Comparison		
		$DSM_{thin\text{-}g}/DSM_{solid}$	$DSM_{thin\text{-}e}/DSM_{solid}$	$DSM_{thin\text{-}g}/AISI$	$DSM_{thin\text{-}e}/AISI$	$DSM_{solid}/AISI$
162 Flange	**Mean**	0.987	0.962	1.024	0.993	1.031
	St Dev	0.049	0.048	0.051	0.048	0.055
250 Flange	**Mean**	0.975	0.956	0.990	0.968	1.057
	St Dev	0.032	0.031	0.001	0.001	0.075
227.5 MPa	**Mean**	0.986	0.963	1.016	0.986	1.031
	St Dev	0.036	0.035	0.039	0.036	0.051
344.7 MPa	**Mean**	0.979	0.956	1.026	0.995	1.038
	St Dev	0.050	0.049	0.061	0.057	0.066
1219 mm	**Mean**	0.962	0.940	1.097	1.061	1.104
	St Dev	0.054	0.052	0.047	0.042	0.045
2438 mm	**Mean**	1.002	0.979	0.997	0.968	1.000
	St Dev	0.009	0.010	0.013	0.015	0.018
All Sections	**Mean**	0.982	0.959	1.021	0.990	1.035
	St Dev	0.044	0.042	0.050	0.046	0.058

The AISI *Specification* provides for the calculation of longwave buckling capacities based on the gross section area for both the punched and unpunched stud. AISI predictions for the perforated stud, however, are often controlled by local buckling which is based on a reduced area at the punchout. DSM results for the equivalent-thickness (perforated) model are therefore compared to AISI predictions for an unperforated (solid) section to reduce the controlling influence of local buckling and provide more direct evaluation.

Perforated Model

For other buckling modes, the perforated web model is used to predict strength at locations of the punchout, where the web no longer consists of a solid plate stiffened on either side, but instead exists as two independent partially stiffened angles. This model is most appropriate, therefore, for buckling modes whose half-wavelength occurs at lengths closer to the length of the perforation. Longwave buckling, however, occurs at a half-wavelength much greater than the perforation length. For this reason, the perforated model used in this study is not applicable for longwave buckling. See the companion paper by Tovar and Sputo (2006) for its application in other limit states.

Comparison of Results

From the normalized DSM/AISI capacity ratios tabulated in Table 4 it appears that the DSM predictions using equivalent-thickness model calculations based on equivalent area come slightly closer to AISI predictions than the same model calculated with gross area. However, each of the models is within the standard deviation of one another and within 0.04 of AISI results. Furthermore, the solid model results are also typically within standard deviation of equivalent thickness and AISI results. It is probably reasonable and prudent within the DSM to simply calculate the longwave buckling capacity for perforated studs based on the solid section.

Conclusions

For the studs considered in this study, it was determined that the solid web model is the most appropriate model for determining longwave buckling strength. In accounting for perforations, the equivalent thickness model has a more accurate distribution of cross-sectional area. However, equivalent thickness predictions fall within one standard deviation of solid web predictions when compared to AISI *Specification* calculated strengths. The use of the equivalent thickness model is, therefore, not recommended.

Appendix. – References

American Iron and Steel Institute (AISI). (2004). *North American Specification for the Design of Cold-Formed Steel Structural Members 2001 Edition with Supplement 2004 (AISI/COFS/NASPEC 2004) and Commentary (AISI/ COFS/NASPEC 2004)*, Washington DC.

Schafer, B.W. (2002a). *Design Manual for Direct Strength Method of Cold-Formed Steel Design, January 2002 Draft.* American Iron and Steel Institute, Washington DC.

Schafer, B.W. (2002b). "Local, distortional, and euler buckling in thin-walled columns." ASCE, *Journal of Structural Engineering*. 128 (3) 289-299.

Sputo, T. and Tovar, J. (2005). "Application of direct strength method to axially loaded perforated cold-formed steel studs: longwave buckling." *Thin Walled Structures,* (43) 1852-1881.

Tovar, J. and Sputo, T. (2006). "Local and distortional buckling of cold-formed steel studs using direct strength." *Proceedings of the 18th International Specialty Conference on Cold-Formed Steel Structures*, Orlando, FL.

Tovar, J. and Sputo, T. (2005). "Application of direct strength method to axially loaded perforated cold-formed steel studs: Distortional and local buckling." *Thin Walled Structures,* (43) 1882-1912.